Supporting Information

A heterobimetallic Pd-Zn complex: Study of a d^8-d^{10} bond in solid state, in solution and in silico

Raphael J. Oeschger, Peter Chen

Laboratorium für Organische Chemie, ETH Zürich, Vladimir-Prelog-Weg 2, 8093 Zürich, Switzerland

peter.chen@org.chem.ethz.ch

Experimental Details

Synthesis and Crystallization of Complex 3

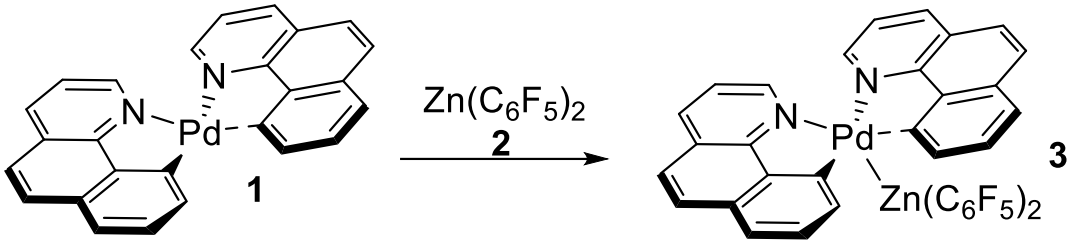

Scheme S1. Preparation of bimetallic complex **3**.

All solvents were dried and distilled prior to use (CH_2Cl_2: CaH_2, 1,2-$C_6H_4F_2$: CaH_2, Hexane: Na/K, Toluene: Na) and stored over molecular sieve in a N_2-filled glovebox. Complex **1** was prepared according to literature[1] procedure and dried at high vacuum prior to use. Complex **2** was purchased from Sigma-Aldrich, purified by crystallization from toluene and dried under high vacuum prior to use.[2]

Bimetallic complex **3** was prepared my mixing a solution of **1** (4.6 mg, 10μM) in 1 mL CH_2Cl_2 with a solution of **2** (4.0 mg, 10μM) in 1 mL 1,2-$C_6H_4F_2$ in a vial in the glovebox. The resulting solution was layered with 0.5 mL of Hexane and put in a glovebox fridge at -35 °C. Colorless crystals were formed overnight.

NMR Experiments

^{1}H NMR and ^{19}F NMR spectra were recorded on a Varian Mercury 300, Varian 500 or a Bruker 600 spectrometer. CD_2Cl_2 was stored over molecular sieve for at least 3 days prior to use. The NMR spectra are reported as follows: chemical shift δ in ppm relative to TMS (δ = 0 ppm), multiplicity, coupling constant (J in Hz), number of protons. The resonance multiplicity is described as s (singlet), d (doublet), t (triplet) or m (multiplet). Broad signals are described with br. (broad).

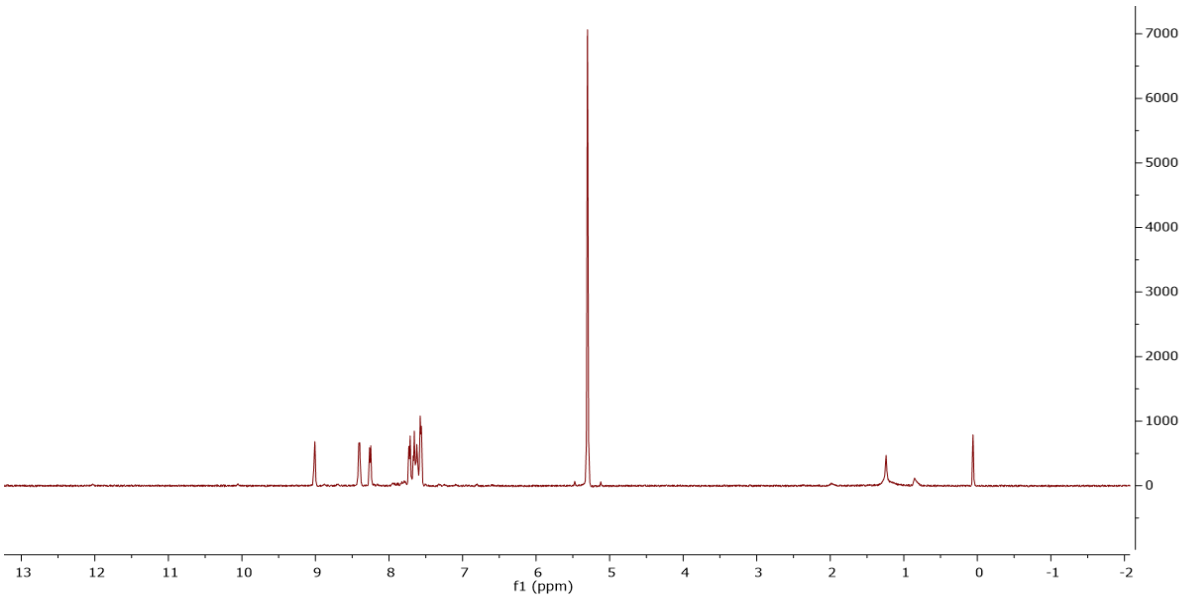

Figure S1. ^{1}H NMR of complex **3** (500 MHz, Methylene Chloride-d2) δ 9.01 (br. d, J = 5.0 Hz, 1H), 8.40 (br. d, J = 7.0 Hz, 1H), 8.26 (br. d, J = 7.9 Hz, 1H), 7.72 (br. d, J = 8.4 Hz, 2H), 7.69 – 7.59 (m, 1H), 7.60 – 7.53 (m, 2H).

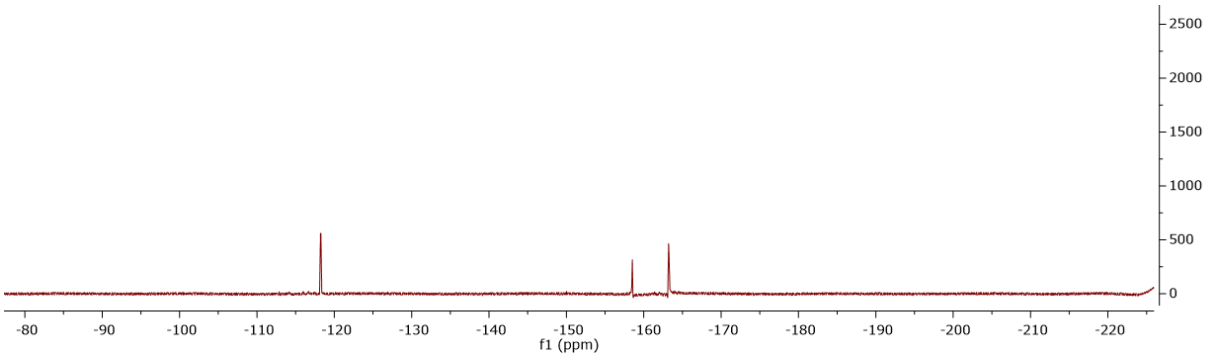

Figure S2. ^{19}F NMR of complex **3** (471 MHz, Methylene Chloride-d2) δ -118.24 (br. d, J = 22.0 Hz), -158.53 (br. t, J = 19.7 Hz), -162.43 – -166.35 (m).

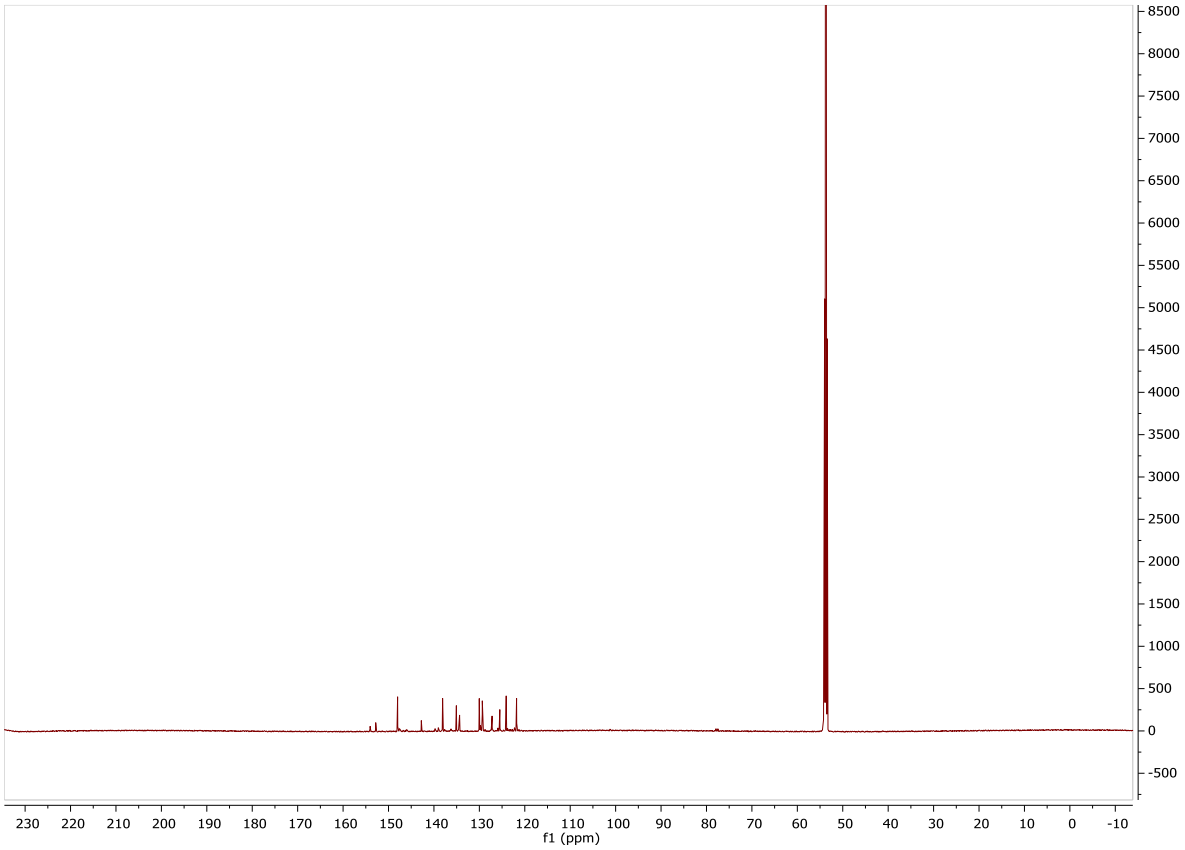

Figure S3. ^{13}C NMR of complex **3** (151 MHz, Methylene Chloride-d2) δ 154.05, 152.82, 148.00, 142.77, 138.09, 135.06, 134.35, 130.02, 129.35, 127.19, 125.50, 124.09, 121.80; (C_6F_5 resonances not observed).

Variable Temperature (VT) NMR Experiments

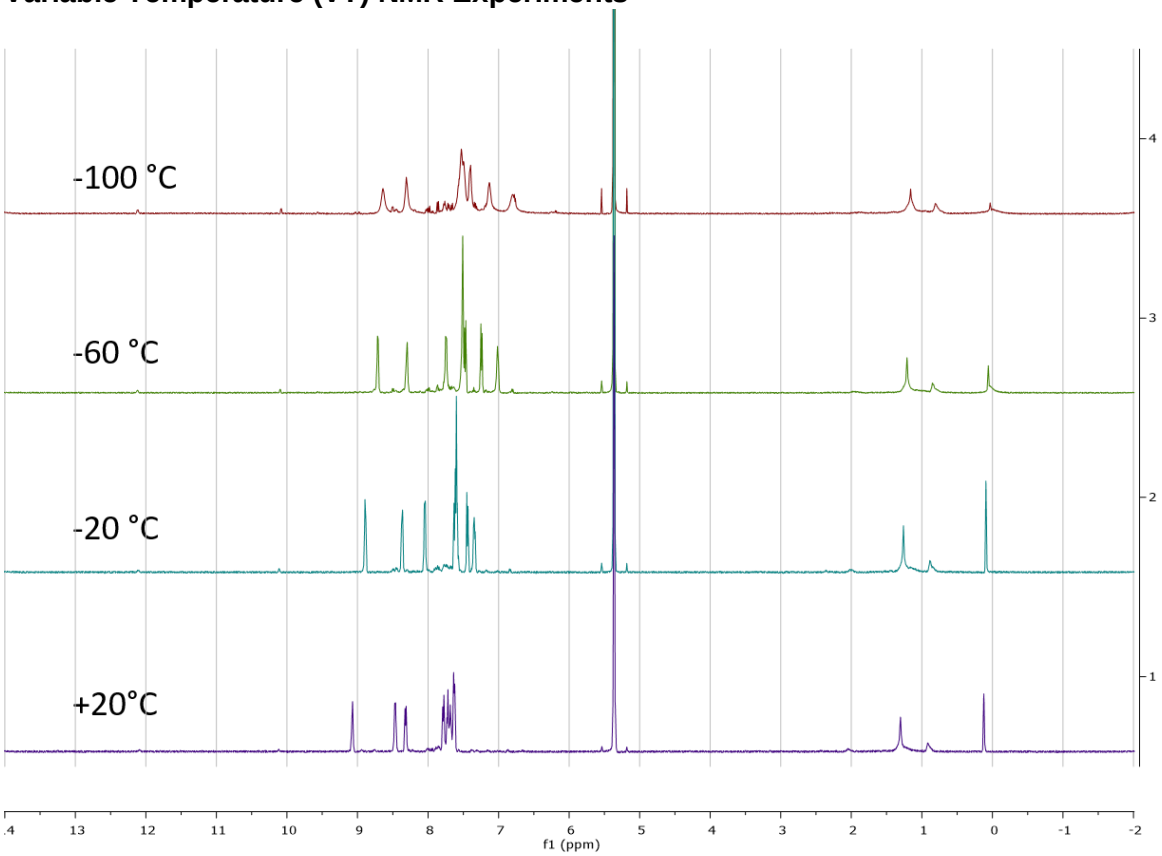

Figure S4. VT-^{1}H NMR spectra (-100 °C to +20 °C) of a solution of **3** in CD_2Cl_2.

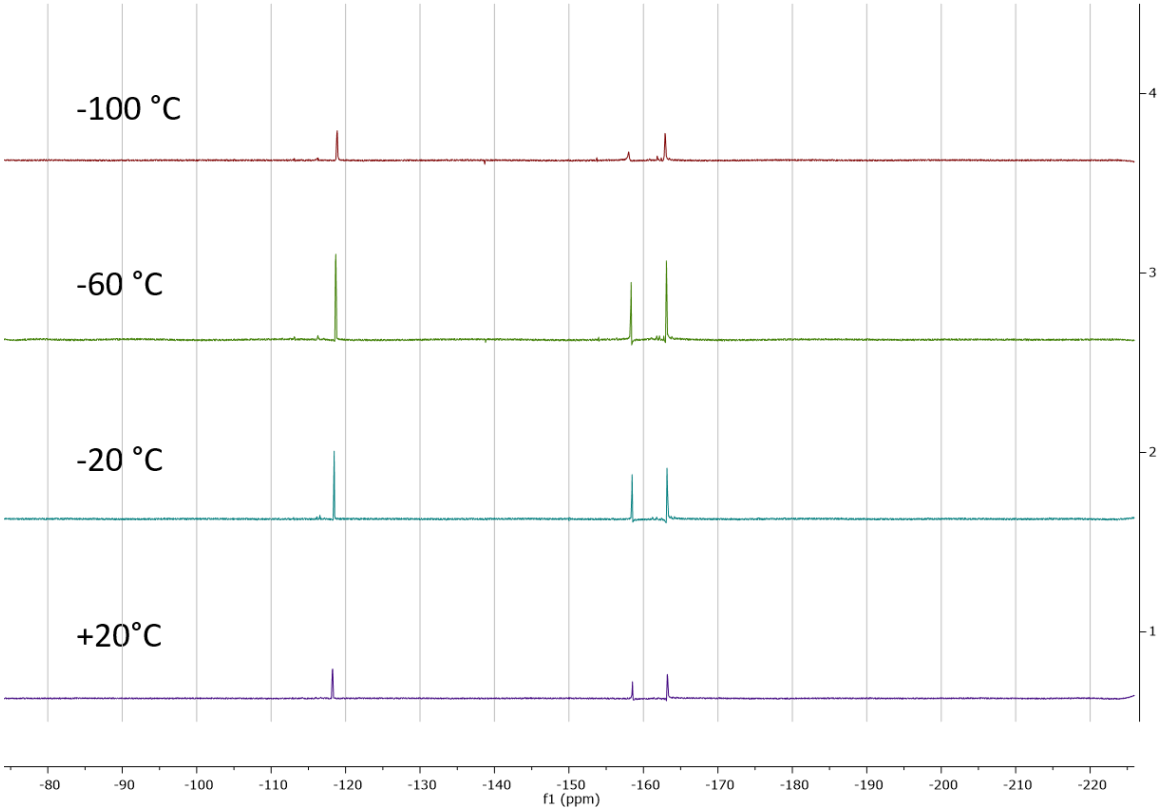

Figure S5. VT-^{19}F NMR spectra (-100 °C to +20 °C) of a solution of **3** in CD_2Cl_2.

NMR-Titration Experiments

A solution of **2** in CD_2Cl_2 (1.663 mM) was prepared in the glovebox. This solution was used to prepare the stock solution of **1**. Exact amounts of the solution of **1** were added by microsyringe to the solution of **2** in a NMR-tube sealed with a septum. A ^{19}F NMR spectrum was recorded after each addition. The change in $\Delta\delta(F_{para})$ was plotted against the concentration of **1**. The data was fitted using the software IGOR Pro 7.01 according to the equation[3]:

$$\Delta\delta = \frac{\Delta\delta_{sat}}{2}\left[\left(\frac{[\mathbf{1}]_0}{[\mathbf{2}]_0} + 1 + \frac{1}{K_a[\mathbf{2}]_0}\right) - \sqrt{\left(\frac{[\mathbf{1}]_0}{[\mathbf{2}]_0} + 1 + \frac{1}{K_a[\mathbf{2}]_0}\right)^2 - 4\frac{[\mathbf{1}]_0}{[\mathbf{2}]_0}}\right]$$

$\Delta\delta$: change in chemical shift, relative to free **2**

$\Delta\delta_{sat}$: Calculated change in chemical shift at saturation

$[\mathbf{2}]_0$: concentration of complex **2** (constant)

[**1**]: concentration of complex **1**

K_a: Association constant (M^{-1})

The error in K_a was estimated to be 20%.

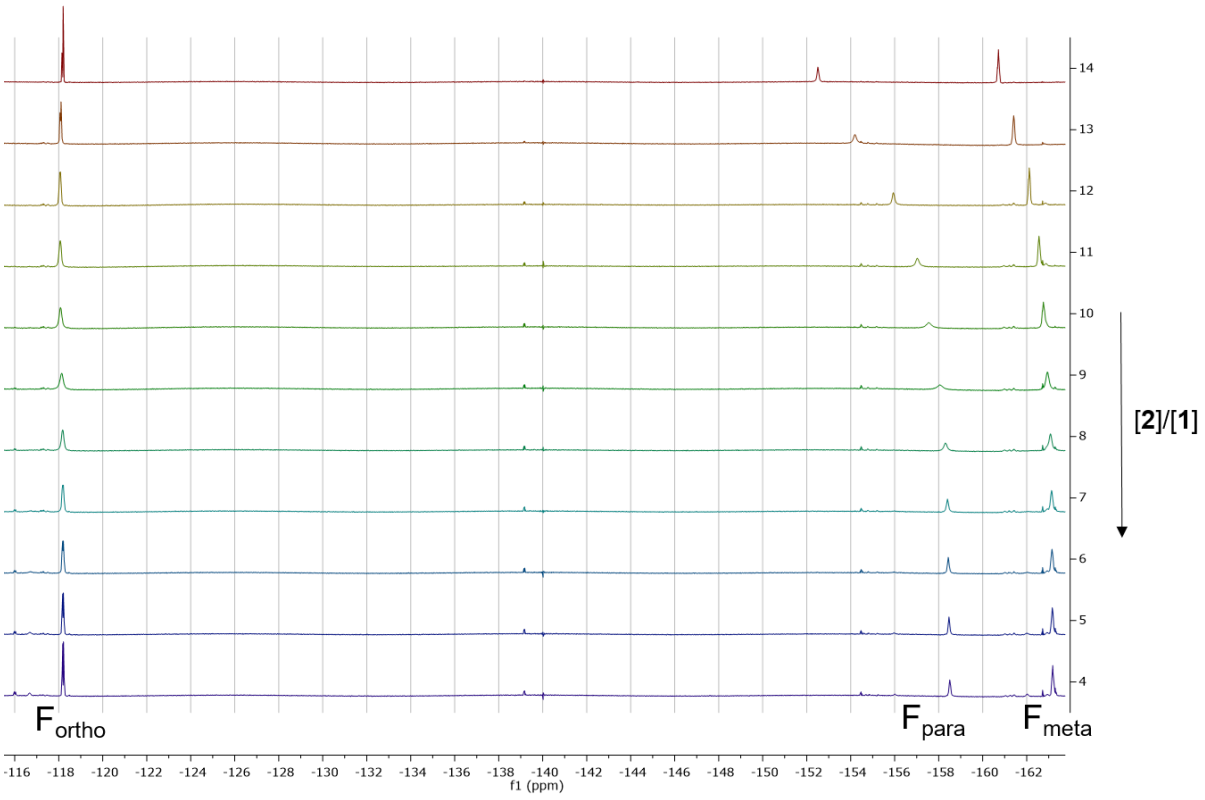

Figure S6. ^{19}F NMR (600 MHz) titration of **1**···**2** in CD_2Cl_2 at 25 °C.

Table S1. ^{19}F NMR-Titration data of **1**···**2** in CD_2Cl_2 at 25 °C.

[**2**] / mol L^{-1}	$\Delta\delta(F_{para})$/ ppm
0	0
0.000506845	1.68
0.000999859	3.44
0.001265242	4.51
0.00139378	5.04
0.001519663	5.55
0.001622596	5.8
0.001723788	5.89
0.001823282	5.93
0.002017344	5.96
0.002386868	5.99
0.002898907	6.03
0.003655603	6.07
0.004666071	6.13

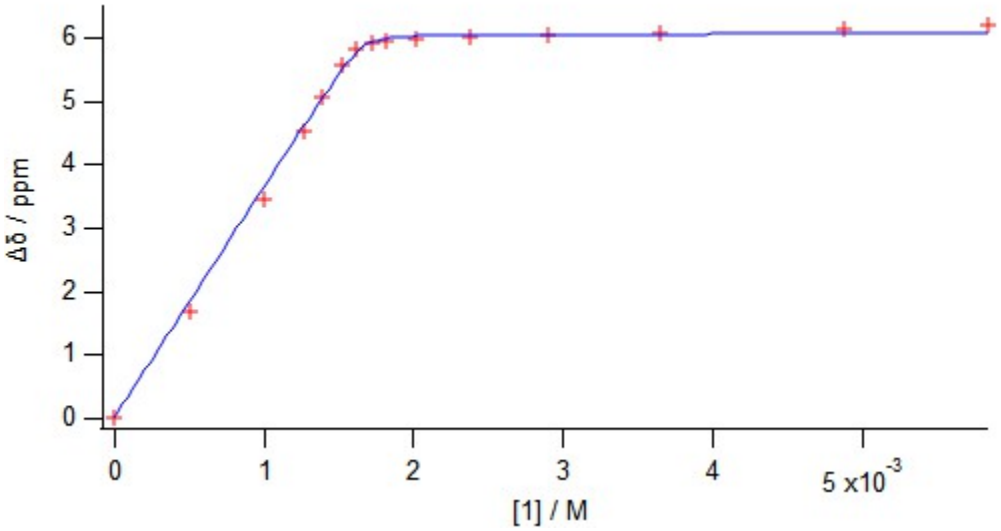

Figure S7.^{19}F NMR binding isotherm of **2** and **1** in CD_2Cl_2 at 25 °C. K_a = (4.5 ± 0.9) × 10^5 mol L^{-1} and δ_{sat} = 6.05 ppm

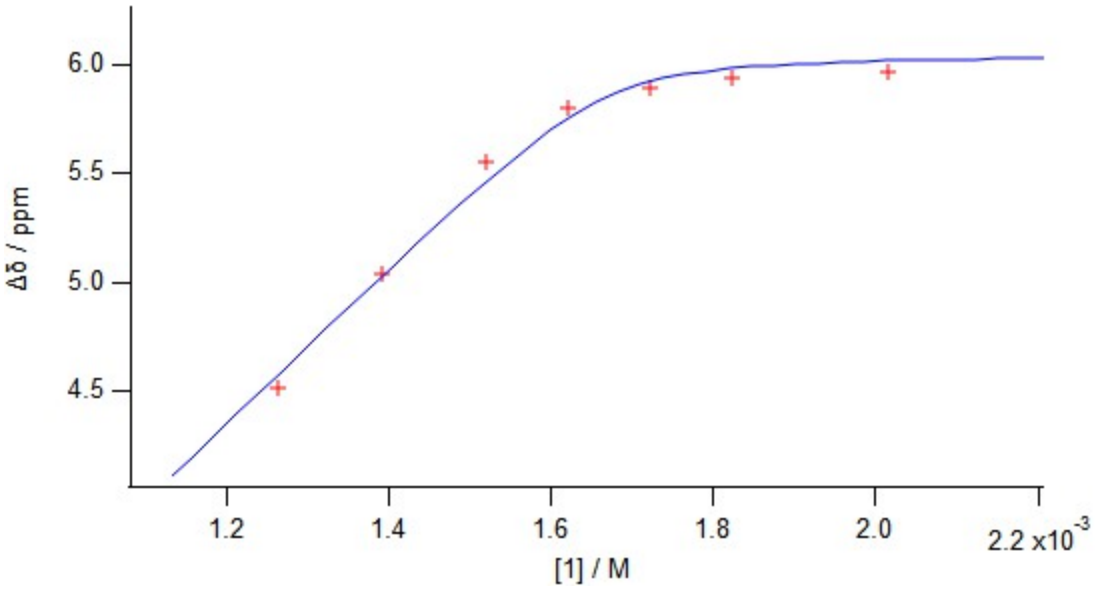

Figure S8. Zoomed-in region of Figure S5.

Elemental Analysis

Table S2. Elemental Analysis (C, H and N) of complex **3**.

C38H16N2F10ZnPd	**[C]**	**[H]**	**[N]**	**[F]**	**[Zn]**	**[Pd]**
Calculated	52.93 %	1.87 %	3.25 %	22.03 %	7.58 %	12.34 %
Found	52.72 %	1.86 %	3.20 %	-	-	-

DFT Calculations

The geometries were optimized using the Gaussian 09 package[4] with TPSS or TPSS-D3 and SDD basis set for Pd,Zn and D95(d,p) basis set on all other atoms. Single point energies were calculated using the TPSS or TPSS-D3 functional and SDD basis set with 2f and g polarization for Pd,Zn, and cc-pVTZ basis set for H,C,N. Table S3 lists the electronic energies of **3** and **1**+**2,** calculated with TPSS vs TPSS-D3, with the geometries of **3** and **1**+**2** optimized with the respective DFT methods. As indicated in Table S5, the optimized geometries differ slightly from each other, and from the x-ray structure.

Table S3. Calculated energy difference between bimetallic complex **3** and **1**+**2** in the gas-phase.

	TPSS /Hartree	**TPSS-D3 /Hartree**
Pd/Zn **3**	-2921.793768	-2921.97223588
$(bhq)_2Pd$ **1**	-1238.413572	-1238.51136927
$Zn(C_6F_5)_2$ **2**	-1683.35747	-1683.39431061
Difference	0.02272618 (16.9 kcal/mol)	0.066556 (41.5 kcal/mol)

The electron density for the AIM analysis was calculated with the coordinates from the crystal structure and the Gaussian09 suite[4] using the TPSS-D3 functional and SDD basis set with 2f and g polarization for Pd,Zn, and cc-pVTZ basis set for H,C,N.

The EDA-NOCV[5] calculations were done with the geometries from the crystal structure. The ADF 2013.01 program package[6] was used with the TPSS-D3 functional and a triple-ζ-quality basis set augmented with one set of polarization functions. Scalar relativistic effects were incorporated by applying the zeroth-order regular approximation (ZORA). The contribution due to dispersion differs slightly from the difference between the TPSS and TPSS-D3 bond energies in Table S3 because of small differences in the geometries used in the calculations. The interaction energy, ΔE_{int}, differs from the bond dissociation energy in Table S3 because ΔE_{int} is the energy needed to dissociate **3** to fragments **1** and **2** fixed at the geometries that they have in **3**.

Table S4. NOCV values in kcal/mol (The percentage values in parentheses give the contribution to the total attractive interactions ($\Delta E_{elstat} + \Delta E_{orb} + \Delta E_{disp}$ = 135.1 kcal/mol). The interaction energy, $\mathbf{\Delta E_{int}}$, is the sum of the attractive interactions and the repulsive Pauli exchange term.

$\mathbf{\Delta E_{int}}$	$\mathbf{\Delta E_{Pauli}}$	$\mathbf{\Delta E_{elstat}}$	$\mathbf{\Delta E_{orb}}$	$\mathbf{\Delta E_{disp}}$
-58.4	76.7	-62.3 (46 %)	-51.1 (38 %)	-21.7 (16 %)

Of the -51.1 kcal/mol orbital interaction energy, -24.8 kcal/mol derive from one pair of interacting orbitals. The next largest contributions are -6.0 and -3.3 kcal/mol. The TPSS-D3 dissociation energy in Table S3, 41.5 kcal/mol, as well as ΔE_{int} in Table S4, -58.4 kcal/mol, greatly exceed the 7.7 kcal/mol dissociation energy measured in CD_2Cl_2 solution. Given that the computed values are for the gas phase, and the experiment is done in polar solvent, one should consider that dielectric shielding should strongly attenuate the attractive electrostatic interaction in solution; the orbital interactions and exchange repulsion should be less strongly affected. Substantial compensation of the attractive dispersion contribution can also be expected in solution. Altogether, the reduction of the gas phase dissociation energy of 41.5 kcal/mol (computed) to 7.7 kcal/mol (experimental) in polar solution is not unexpected.

Comparison of selected bond lengths and angles in bimetallic complex 3

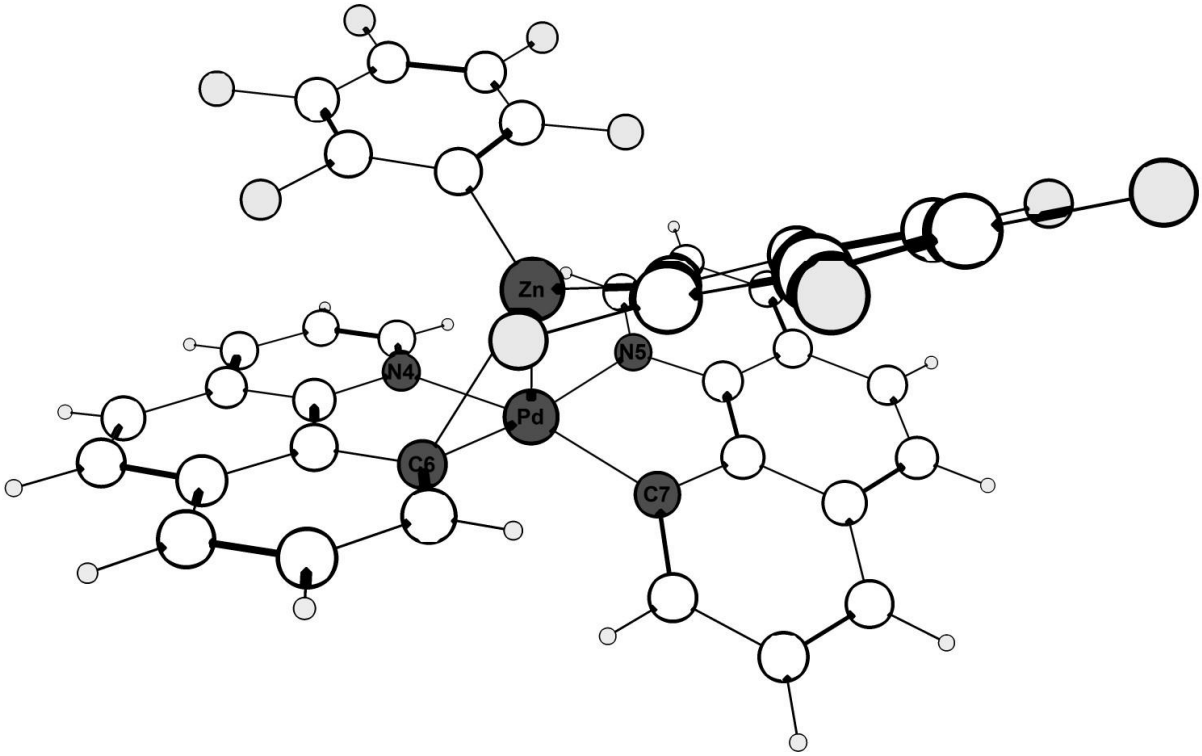

Figure S9. Crystal Structure of bimetallic complex **3**.

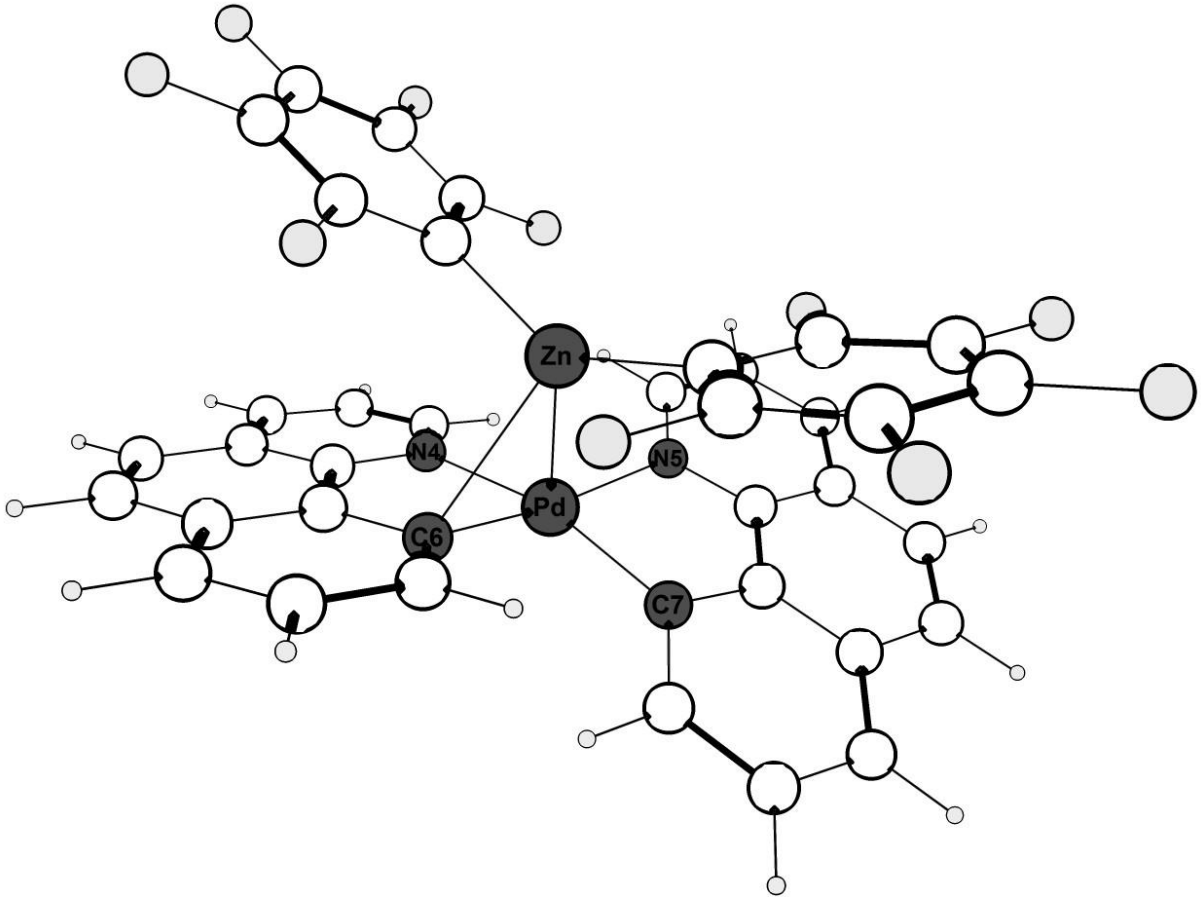

Figure S10. DFT (TPSS) optimized structure of bimetallic complex **3**.

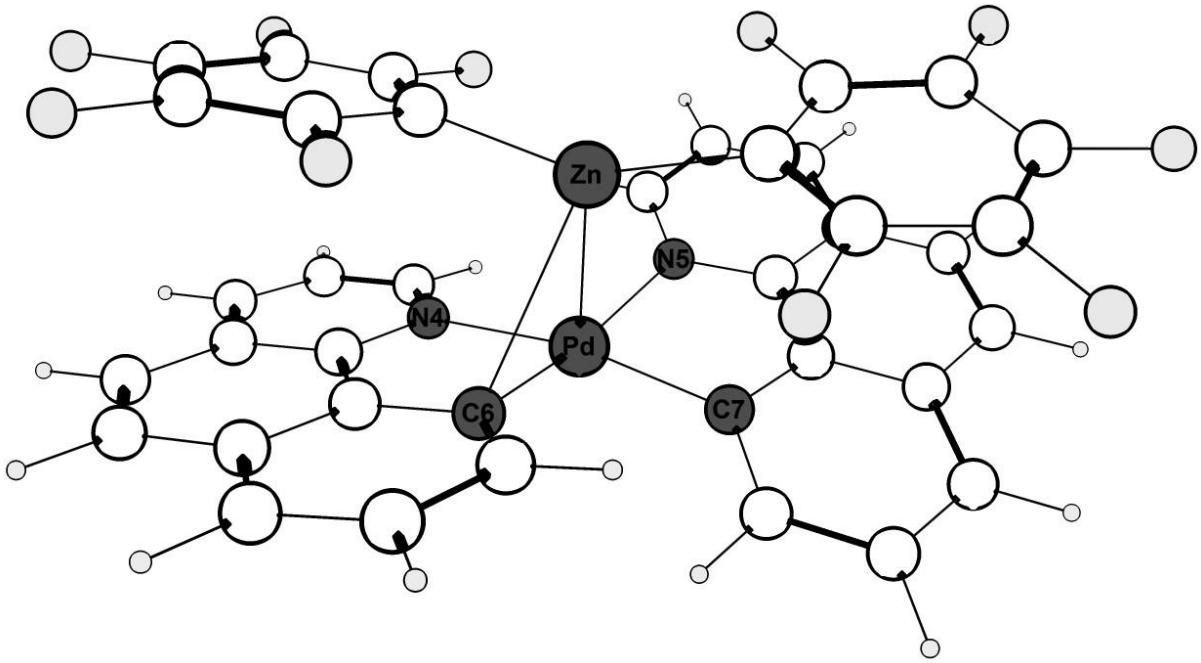

Figure S11. DFT (TPSS-D3) optimized structure of bimetallic complex **3**.

Table S5. Comparison of selected bond lengths (Å) and angles (°).

Bond (Å) / Angle (°)	***X-Ray***	***TPSS***	***Difference***	***TPSS-D3***	***Difference***
Pd-Zn	2.579	2.654	0.075	2.623	0.044
Pd-C6	2.031	2.032	0.001	2.021	-0.01
Pd-C7	1.997	2.013	0.016	2.008	0.011
Pd-N4	2.158	2.176	0.018	2.158	0
Pd-N5	2.141	2.156	0.015	2.158	0.017
Zn-C6	2.473	2.632	0.159	2.869	0.396
N5-Pd-C6	166.1	168.6	2.5	165.9	-0.2
N4-Pd-C7	167.6	163.9	-3.7	167.4	-0.2
N5-Pd-Zn	102.5	101.8	-0.7	90.9	-11.6

XYZ-Coordinates of X-Ray Structure of Complex 3

Pd-Zn (3) (E = -2921.71489447 a.u.)

Pd	3.808146000	5.063968000	4.632680000
Zn	2.286856000	5.339158000	6.696367000
F	-0.805831000	6.359587000	6.997888000
F	1.700592000	2.351043000	6.903185000
F	4.106605000	3.401695000	8.199354000
F	3.655224000	8.093839000	7.862748000
F	-3.011691000	4.954210000	7.599214000
F	-0.525459000	0.954813000	7.476812000
F	6.435509000	3.718640000	9.510427000
F	6.012125000	8.398456000	9.124491000
F	-2.871663000	2.261169000	7.930940000
F	7.416314000	6.236308000	9.954135000
N	5.362703000	6.510305000	5.069133000
N	4.758037000	3.180986000	5.004107000
C	5.533075000	0.528905000	5.453881000
H	5.817968000	-0.365859000	5.588550000
C	2.670278000	6.744534000	4.697838000
C	2.427029000	3.868961000	3.823877000
C	0.548819000	4.415363000	6.937874000
C	3.802261000	5.732059000	7.939645000
C	6.676067000	6.347259000	5.225828000
H	7.022872000	5.464027000	5.252208000
C	4.879586000	7.784847000	5.010965000
C	3.962700000	2.142264000	4.609861000
C	5.884626000	2.883925000	5.648432000
H	6.430045000	3.598941000	5.957866000
C	3.461704000	7.921248000	4.852819000
C	1.284913000	6.934622000	4.672381000
H	0.714697000	6.179838000	4.599309000
C	1.344218000	4.181532000	3.008478000
H	1.125431000	5.094191000	2.852970000
C	2.742092000	2.493807000	3.954720000
C	-0.679072000	5.007498000	7.127017000
C	0.540870000	3.035040000	7.073202000
C	4.552656000	4.668283000	8.412106000
C	4.329466000	6.971208000	8.235230000
C	7.567297000	7.419385000	5.352715000
H	8.495056000	7.257532000	5.479074000
C	5.710854000	8.913443000	5.134686000
C	4.319930000	0.796141000	4.803357000
C	6.303446000	1.571206000	5.892049000
H	7.114387000	1.403786000	6.357520000
C	2.900929000	9.213686000	4.890014000
C	0.713521000	8.220696000	4.753103000
H	-0.231498000	8.311366000	4.748355000
C	0.566918000	3.171442000	2.410054000
H	-0.152762000	3.416011000	1.839988000
C	1.936040000	1.469402000	3.416573000
C	-1.828884000	4.323501000	7.455313000
C	-0.578310000	2.298948000	7.385406000
C	5.752772000	4.798322000	9.080965000
C	5.529028000	7.160898000	8.891163000
C	7.090729000	8.699892000	5.293229000
H	7.686465000	9.436780000	5.357727000
C	5.109718000	10.213833000	5.101448000
H	5.659431000	10.987705000	5.149327000
C	3.431345000	-0.227469000	4.313089000
H	3.643637000	-1.141322000	4.456859000
C	3.766377000	10.351826000	5.002128000
H	3.388456000	11.222332000	5.006876000
C	1.492650000	9.338157000	4.837650000
H	1.090222000	10.196336000	4.861788000
C	0.827538000	1.849975000	2.633490000
H	0.260273000	1.185066000	2.260745000
C	2.301841000	0.099418000	3.651221000
H	1.734309000	-0.592533000	3.333081000
C	-1.768990000	2.949541000	7.602908000
C	6.248848000	6.060139000	9.310601000

References

(1) Jolliet, P.; Gianini, M.; von Zelewsky, A.; Bernardinelli, G.; Stoeckli-Evans, H., *Inorg. Chem.* **1996,** *35*, 4883-4888.
(2) Guerrero, A.; Martin, E.; Hughes, D. L.; Kaltsoyannis, N.; Bochmann, M., *Organometallics* **2006,** *25*, 3311-3313.
(3) Biedermann, F.; Schneider, H.-J., *Chem. Rev.* **2016,** *116*, 5216-5300.
(4) Frisch, M. J.; Trucks, G. W.; Schlegel, H. B.; Scuseria, G. E.; Robb, M. A.; Cheeseman, J. R.; Scalmani, G.; Barone, V.; Mennucci, B.; Petersson, G. A.; Nakatsuji, H.; Caricato, M.; Li, X.; Hratchian, H. P.; Izmaylov, A. F.; Bloino, J.; Zheng, G.; Sonnenberg, J. L.; Hada, M.; Ehara, M.; Toyota, K.; Fukuda, R.; Hasegawa, J.; Ishida, M.; Nakajima, T.; Honda, Y.; Kitao, O.; Nakai, H.; Vreven, T.; Montgomery, J. A.; Peralta, J. E.; Ogliaro, F.; Bearpark, M.; Heyd, J. J.; Brothers, E.; Kudin, K. N.; Staroverov, V. N.; Kobayashi, R.; Normand, J.; Raghavachari, K.; Rendell, A.; Burant, J. C.; Iyengar, S. S.; Tomasi, J.; Cossi, M.; Rega, N.; Millam, J. M.; Klene, M.; Knox, J. E.; Cross, J. B.; Bakken, V.; Adamo, C.; Jaramillo, J.; Gomperts, R.; Stratmann, R. E.; Yazyev, O.; Austin, A. J.; Cammi, R.; Pomelli, C.; Ochterski, J. W.; Martin, R. L.; Morokuma, K.; Zakrzewski, V. G.; Voth, G. A.; Salvador, P.; Dannenberg, J. J.; Dapprich, S.; Daniels, A. D.; Farkas; Foresman, J. B.; Ortiz, J. V.; Cioslowski, J.; Fox, D. J., Gaussian 09, Revision D.01. Wallingford CT, 2009.
(5) Mitoraj, M. P.; Michalak, A.; Ziegler, T., *Journal of Chemical Theory and Computation* **2009,** *5*, 962-975.
(6) ADF2013, S., Theoretical Chemistry, Vrije Universiteit, Amsterdam, The Netherlands, http://www.scm.com.